Glycobiology vol. 22 no. 7 pp. 918–929, 2012
doi:10.1093/glycob/cws060
Advance Access publication on March 14, 2012

O-Linked glycome and proteome of high-molecular-mass proteins in human ovarian cancer ascites: Identification of sulfation, disialic acid and *O*-linked fucose

Niclas G Karlsson[1,2] and Michael A McGuckin[3]

[2]Medical Biochemistry, University of Gothenburg, PO Box 440, 405 30 Gothenburg, Sweden and [3]Immunity, Infection and Inflammation Program, Mater Medical Research Institute and The University of Queensland, Level 3 Aubigny Place, Mater Health Services, South Brisbane, QLD 4101, Australia

Received on November 2, 2011; revised on March 5, 2012; accepted on March 5, 2012

The *O*-linked glycosylation of the main acidic high-molecular-weight glycoprotein from ascites fluid from patients with ovarian cancer were analyzed. The *O*-linked oligosaccharides were shown to consist of mainly highly sialylated core 1 and 2 structures with a smaller amount of sulfated core 2 structures. These structures were shown to be able to be further extended into small keratan sulfate (KS)-type oligosaccharides with up to four *N*-acetyllactosamine units. Proteomic studies of the acidic fraction of ascites fluid from patients with ovarian cancer showed that this fraction was enriched in proteoglycans. Among them, lumican, agrin, versican and dystroglycans were potential candidates, with threonine- and serine-rich domains that could carry a significant amount of *O*-linked glycosylation, including also the *O*-linked KS. Glycomic analysis using liquid chromatography (LC)-tandem mass spectrometry (MS/MS) also showed that the disialic acid NeuAc-NeuAc- was frequently found as the terminating structure on the *O*-linked core 1 and 2 oligosaccharides from one ascites sample. Also, a small amount of the epidermal growth factor (EGF)-associated *O*-linked fucose structure Gal-GlcNAc-Fucitol was detected with and without sialic acid in the LC-MS/MS analysis. Candidate proteins containing *O*-linked fucose were suggested to be proteoglycan-type molecules containing the *O*-linked fucose EGF consensus domain.

Keywords: CA125 / keratan sulfate / mass spectrometry / *O*-linked oligosaccharides / proteoglycan

Introduction

O-Linked glycosylation is one of the most ubiquitous and most important post-translational modifications of proteins and is connected to the biological roles such as fertilization (Pang et al. 2011), cancer (Brockhausen 2006) and inflammation (McEver 1997; Estrella et al. 2010). Studying the *O*-linked glycome is essential for making the connections between structure and function and how an altered glycosylation machinery participates in disease etiology. These connections will also provide the biological relevance for glycobiomarker discovery and the cataloguing of oligosaccharide structures on complex glycoproteins that is now possible using mass spectrometry-based techniques. *O*-Linked oligosaccharides are mostly known in the area of mucins, where mucosal surfaces are protected by heavily glycosylated (up to 80% of the weight) proteins belonging to the mucin family (MUC1–20), constituting the major macromolecular component of mucus and the mucosal apical glycocalyx (Lindén et al. 2008). The mucin-type glycosylation is initiated in the Golgi/endoplasmic reticulum (ER) by the attachment of GalNAc to Ser or Thr residues by a family of GalNAc transferases (Tarp and Clausen 2008). The GalNAc moieties are then further extended on the C-3 and C-6 carbon by *N*-acetyllactosamine (LacNAc) extensions and/or terminated by blood group antigens, sialylation and sulfation. The mucin-type glycosylation is also prevalent on many other secreted glycoproteins that are synthesized in the ER and Golgi and secreted via the classical secretory pathway. The plasma *O*-linked oligosaccharides are dominated by short sialylated structures (sialyl and di-sialyl-T; Wilson et al. 2002), whereas, for instance, *O*-linked keratan sulfate (KS) proteoglycans in the extracellular matrix consist of extended poly-sulfated poly-LacNAc oligosaccharides (Zaia 2009).

Although alteration in *O*-linked glycosylation is one of the hallmarks for cancer, this is usually accompanied by an altered differentiation state and environment of the cancer cells. These alterations may not only be regulated by the genome via altered expression of glycosyltransferase and mucin genes, but also due to an altered Golgi apparatus and secretory pathway (Axelsson et al. 2001; Gill et al. 2010). Ovarian cancer is one of the cancers with highest incidence and fatalities in the Western world, and early detection of ovarian cancer is one of the key factors for successful treatment. The mucin MUC16 measured as CA125 is the gold

[1]To whom correspondence should be addressed: Tel: +46-31-786-6528; Fax: +46-31-41-6108; e-mail: niclas.karlsson@medkem.gu.se

© The Author 2012. Published by Oxford University Press. All rights reserved. For permissions, please e-mail: journals.permissions@oup.com

Downloaded from https://academic.oup.com/glycob/article/22/7/918/1988054 by guest on 21 August 2022

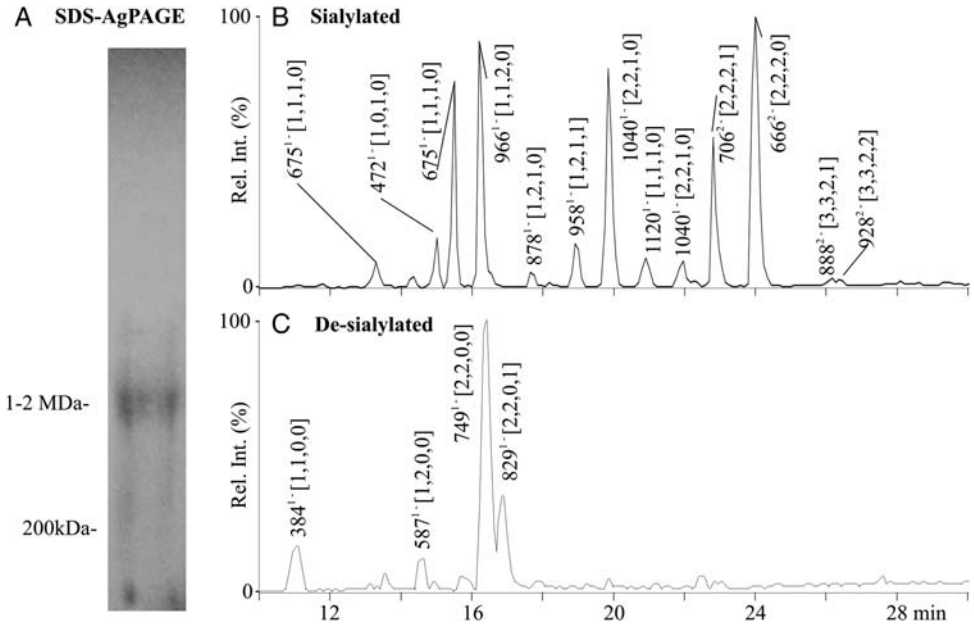

Fig. 1. Glycosylation of high-molecular-mass protein from patients with ovarian cancer. Alcian blue stain (sialic acid and sulfate) after SDS–AgPAGE of acidic proteins in ascites (**A**), and base peak chromatogram from LC-MS of oligosaccharides released from the Alcian blue stained area before (**B**) and after (**C**) desialylation. Oligosaccharide alditol compositions are referred to as (Hex, HexNAc, NeuAc, sulfate), showing dominant compositions corresponding to core 1 (1, 1, 0–2, 0) and core 2 (1–2, 2, 0–2, 0–1).

standard for monitoring the efficacy of ovarian cancer therapy (Karam and Karlan 2010), but its use in ovarian cancer screening diagnosis has not been successful due to its low specificity. Other glycosylation-dependent markers, such as CA19.9, CA50 and CA242, are also used as serum markers for cancer (Chauhan et al. 2009). Most of these assays are based on the antibody recognition of the oligosaccharide structures without distinction between different glycoproteins on which they may be carried. *N*-Linked glycosylation expressing sialyl-Lewis^x on common plasma proteins has also been suggested to increase the sensitivity of ovarian cancer diagnostics (Saldova et al. 2008). Despite the potential of a combined protein/oligosaccharide for the diagnosis of ovarian cancer, the methodology to identify glycobiomarkers is not straightforward, and only dedicated glycoanalytical research groups are successfully pursuing this pathway. This point is exemplified by the only detailed characterization of oligosaccharides from the ovarian cancer antigen CA125 being restricted to ovarian cell lines (Kui Wong et al. 2003), whereas the knowledge of *O*-linked glycosylation of CA125 from primary ovarian cancers is currently based only on lectin/antibody recognition.

We have developed a platform for the analysis of *O*-linked oligosaccharides based on the isolation of high-molecular-weight acidic glycoproteins and analysis using negative-ion graphitized carbon liquid chromatography (LC) coupled to mass spectrometry (Schulz et al. 2002). This platform has been shown to address the questions of individual variation in glycosylation (Thomsson et al. 2005) as well as identifying disease-related differences in *O*-linked glycosylation in cystic fibrosis (Holmén et al. 2004; Schulz et al. 2004, 2007), ulcerative colitis (Larsson et al. 2011) and differences in glycosylation between rheumatoid arthritis and osteoarthritis (Estrella et al. 2010). Using this platform, we set out to address the *O*-linked glycosylation of large glycoproteins present in the ascites from one patient with papillary serous adenocarcinoma. Using this result, we also queried other ovarian cancer ascites samples to identify commonalities in *O*-linked glycosylation and the secreted glycoproteome.

Results

Sialylated oligosaccharide detected from acidic high-molecular-weight proteins of ovarian cancer ascites

Acidic proteins from ascites from a patient with papillary serous adenocarcinoma (SER8, Supplementary data, Tables S1 and S2, Figure S1, CA125 negative) were isolated by anion-exchange chromatography. In order to identify sialylated and/or sulfated high-molecular-mass glycoproteins, the acidic proteins from DEAE Sephadex were subjected to sodium dodecyl sulfate–polyacrylamide/agarose composite gel electrophoresis (SDS–AgPAGE), where mucins and other large glycoproteins from 100 kDa to 10 MDa can be separated (Schulz et al. 2002). One major band with an apparent mass of >1 MDa was detected using Alcian blue (Figure 1), indicating that there were highly acidic oligosaccharides present, containing either sialic acid, sulfate or both. This observation could be verified after subjecting this region of the gel to reductive β-elimination and analyzing released oligosaccharides by LC-tandem mass spectrometry (MS/MS). It was found that the LC-MS profile was dominated by mono- and disialylated core 1 structures ([M–H] ions of *m/z* 675 and 966) and core 2 structures ([M–H]$^-$ ion of *m/z* 1040 and [M–H]$^-$/[M–H]$^{2-}$

Downloaded from https://academic.oup.com/glycob/article/22/7/918/1988054 by guest on 21 August 2022

Table I. Low-molecular-weight oligosaccharides identified by LC-MS from Alcian blue stained band in Fig. 1 after release by reductive β-elimination

$[M–nH]^{n-}$	Structure[a]	Retention time	Ion intensity (%)
384^-	Galβ1-3GalNAc	8.7	0.7
425^-	GlcNAcβ1-3GalNAcol	13.2	0.5
513^-	**NeuAcα2-6**GalNAcol	11.8	0.2
587^-	Galβ1-3(**GlcNAcβ1-6**)GalNAcol	13.6	0.2
667^-	Galβ1-3(**HSO_3-6GlcNAcβ1-6**)GalNAcol	14.8	0.2
675^-	Galβ1-3(**NeuAcα2-6**)GalNAcol	13.3	1.5
675^-	NeuAcα2-Galβ1-3GalNAcol	15.5	6.5
749^-	Galβ1-3(**Galβ1-4GlcNAcβ1-6**)GalNAcol	16.5	1.2
966^-	NeuAcα2-Galβ1-3(**NeuAcα2-6**)GalNAcol	16.2	15.9
829^-	Galβ1-3(**Galβ1-4(HSO_3-6)GlcNAcβ1-6**)GalNAcol	17.0	0.2
878^-	NeuAcα2-Galβ1-3(**GlcNAcβ1-6**)GalNAcol	17.6	0.5
958^-	NeuAcα2-Galβ1-3(**HSO_3-6GlcNAcβ1-6**)GalNAcol	18.9	5.3
1040^-	NeuAcα2-Galβ1-3(**Galβ1-4GlcNAcβ1-6**)GalNAcol	19.8	15.3
1120^-	NeuAcα2-Galβ1-3(**Galβ1-4(HSO_3-6)GlcNAcβ1-6**)GalNAcol	20.9	3.2
1120^-	Galβ1-3(**NeuAcα2-Galβ1-4(HSO_3-6)GlcNAcβ1-6**)GalNAcol	21.9	1.0
666^{2-}	NeuAcα2-Galβ1-3(**NeuAcα2-Galβ1-4GlcNAcβ1-6**)GalNAcol	24.0	36.3
666^{2-}	NeuAcα2-Galβ1-GlcNAcβ1-Galβ1-3(**NeuAcα2-6**)GalNAcol	25.6	0.1
706^{2-}	NeuAcα2-Galβ1-3(**NeuAcα2-Galβ1-4(HSO_3-6GlcNAcβ1-6**)GalNAcol	22.8	10.5
706^{2-}	$HSO_3NeuAc_2Gal_2GlcNAc_1GalNAcol_1$	25.6	0.3
851^{2-}	NeuAcα2-Galβ1-3(**NeuAcα2-Galβ1-4(HSO_3-6)GlcNAcβ1-6**)GalNAcol + NeuAc	21.4	0.1
1257^-	NeuAcα2-Galβ1-3(**NeuAcα2-6**)GalNAcol + NeuAc	17.2	0.1
530^-	Galβ1-GlcNAcβ1-Fucol	17.4	0.0
821^-	NeuAcα2-Galβ1-GlcNAcβ1-Fucol	23.6	0.2

Associated fragment spectra were submitted to Unicarb-DB (Hayes et al. 2011; www.unicarb-DB.com).
[a]Linkage configuration and position based on core 1, 2 and 3 series of extension. Type 2 configuration Galβ1-4GlcNAcβ1- is based on the detection of linkage-specific MS/MS fragment of desialylated structures. Six-linked sialic acid assigned from the detection of sialic acid directly linked to GalNAc. Sulfation is assumed to be C-6 on GlcNAc residues. C-6 branch of GalNAcol is bold to help reading of sequences.

ions of *m/z* 1331/666; Table I). Low-intense, low-molecular mass ions were also detected ($[M–H]^-$ ion of *m/z* 513), which the MS/MS fragmentation showed corresponded to the sialyl-Tn structure NeuAcα2-6GalNAcol (Table I). There were no compositions of mucin-type fucosylated structures detected. This indicated that previously described cancer-associated fucose-containing oligosaccharide structures, such as sialyl-Lewis^x or sialyl-Lewis^a (CA19-9), were not major components of the *O*-linked oligosaccharides in the major high Mr component of this sample.

In order to confirm the sequence of the intense core 2 structure, the sample was desialylated and the dominating $[M–H]^-$ ion of *m/z* 749 in the chromatogram (Figure 1C), corresponding to the sequence of a core 2, type 2 tetrasaccharide Galβ1-4GlcNAcβ1-6(Galβ1-3)GalNAcol, was identified by MS/MS (Figure 2).

Sulfation of human ascites oligosaccharides

Having identified that the dominating peaks of the oligosaccharides released from the >1 MDa Alcian blue stained band (Figure 1A) were sialylated core 1 and 2 structures, LC-MS/MS of the minor components showed that ovarian cancer ascites oligosaccharides also contained parent ions corresponding to sulfated structures such as the $[M–H]^-$ ion of *m/z* 1120 and the $[M–H]^-/[M–H]^{2-}$ ion pair of *m/z* 1411/706. These masses corresponded to the sulfated versions of the identified sialylated core 2 structures (Table I; MS/MS of $[M–H]^{2-}$ ion of *m/z* 706 in Figure 3A). In order to confirm this assignment and to identify the location of the sulfate, further analysis was performed. The $[M–H]^-$ ion of monosialylated monosulfated *m/z* 1120 (two components) and disialylated monosulfated $[M–H]^-/[M–H]^{2-}$ ions *m/z* 1411/706 (single component) were detected after desialylation in the LC-MS chromatogram as one single LC-MS peak with an $[M–H]^-$ ion of *m/z* 829. The MS/MS (Figure 3B) of this ion confirmed that this was a core 2 tetrasaccharide modified by sulfation (Table I). The location of sulfate was shown to be on the GlcNAc on the C-6 branch of the GalNAcol, indicated by the fragment $Y_{1\alpha}/Y_{1\beta}$ of *m/z* 505 and $Y_{1\alpha}/C_{1\alpha}$ or $Z_{1\alpha}/B_{1\alpha}$ of *m/z* 282.

Further analysis of the of the LC chromatogram showed that the disialylated sulfated core 2 structure ($[M–H]^-/[M–H]^{2-}$ ion pair of *m/z* 1411/706) was the first structure in a series of structures extended by sulfated LacNAc units (Figure 4). Doubly charged ions displayed a complex sulfation of core 2 structures extended with up to three LacNAc units, with the maximum sulfation of one sulfate per LacNAc unit. This indicated that, rather than classical mucin-type oligosaccharides, the glycosylation of this sample were extended into shorter KS-type structures. The sulfation attached to GlcNAc in the first structure of this series further strengthens this argument, since KS is dominated by 6-linked sulfate to GlcNAc. Due to the low intensity of the $[M–2H]^{2-}$ ions in Figure 4B–D, the fragmentation could confirm that it was consistent with the assigned monosaccharide composition, but the sites of sulfation could not be identified.

Downloaded from https://academic.oup.com/glycob/article/22/7/918/1988054 by guest on 21 August 2022

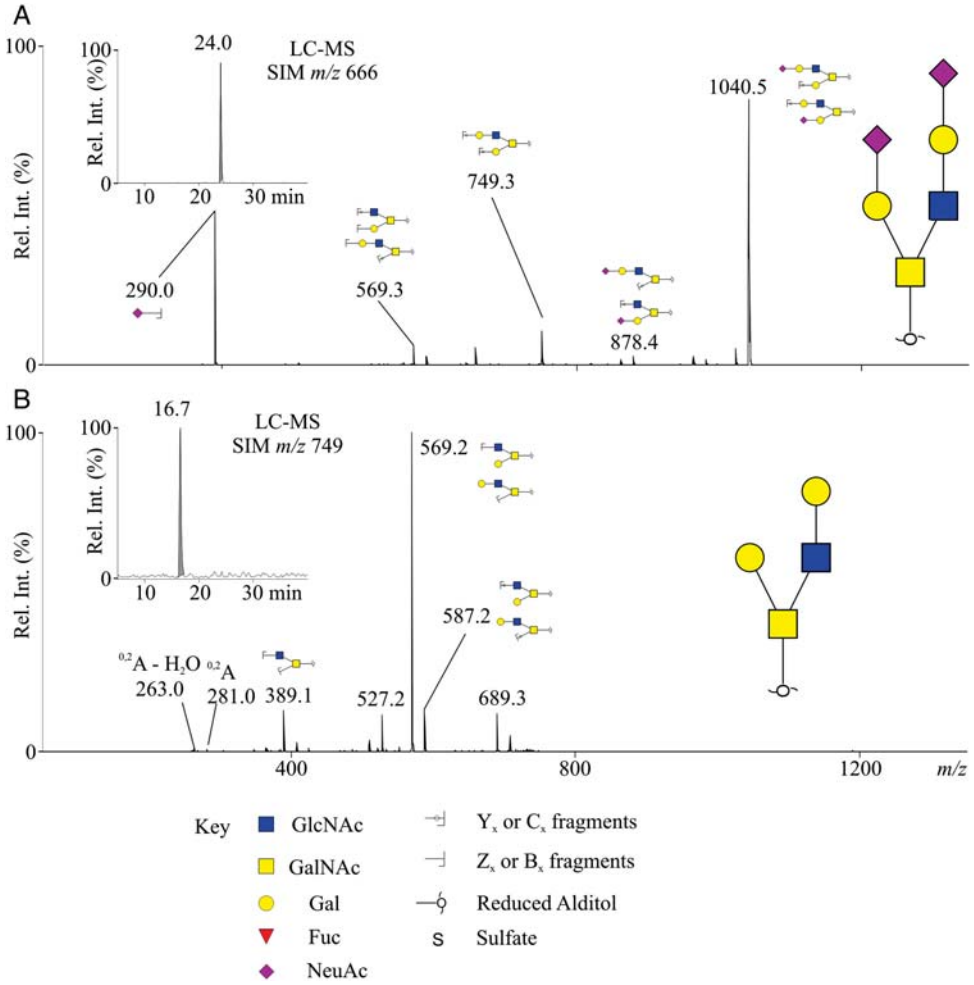

Fig. 2. Identification of sialylated core 2 structure NeuAc2-Gal1-4GlcNAc1-6(NeuAc2-Gal1-3)GalNAcol from ovarian ascites. The MS/MS spectrum of the $[M–2H]^{2–}$ ion of *m/z* 666 eluted at retention time (RT) 24.0 min before (**A**) and that of the $[M–H]^{–}$ ion of *m/z* 749 eluted at RT 16.7 min after (**B**) desialylation. Inserted are selected ion chromatograms (SIM) of each ion, respectively. ^{0,2}A fragment of *m/z* 281 and ^{0,2}A – H_2O of *m/z* 263 shown to be specific for the type 2 (Galβ1-4GlcNAc) and not type 1 (Galβ1-3GlcNAc) chains (Schulz et al. 2002) is specifically labeled in (B).

Detection of the NeuAc-NeuAc motif in human ascites oligosaccharides

With sensitive detection of oligosaccharides by LC-MS, the method is also capable of detecting less common *O*-linked motifs. Selected fragment ion MS/MS chromatograms showed that the theoretical negative-ion B_2 fragment of *m/z* 581 of two sialic acids linked together was present in the sample. MS/MS were generated of two structures corresponding to a trisialylated core 1 structure of $[M–H]^{–}$ ion of *m/z* 1257 with the composition $NeuAc_3Hex_1HexNAc_1$-ol and of the trisialylated sulfated core 2 structure ($[M–H]^{–}/[M–H]^{2–}$ ion pair of *m/z* 1702/851) with the composition HSO_3-$NeuAc_3Hex_2HexNAc_2$ (Figure 5A). Both these parent ions gave intense B_2 fragment ions of *m/z* 581 (Figure 5B and C). After desialylation, the HSO_3-$NeuAc_3Hex_2HexNAc_3$ structure was shown to have the same core as the one described in the beginning of this section, since only one isomer of the $[M–H]^{–}$ ion of *m/z* 829 corresponding to the desialylated sulfated core 2 could be detected. These data indicate that the disialic acid motif was an extension of the sialylated structures present in high abundance in the sample (Table I) and was a common motif in this sample (Figure 5A).

In order to investigate the involvement of disialylation on the surface of ovarian cancer cells, the presence of *O*-linked oligosaccharides from ovarian cancer tissue was investigated after the enrichment of membrane-associated proteins (Pedersen et al. 2003). The enrichment of membrane proteins and release of *O*-linked oligosaccharides from a patient with ovarian cancer showed that the disialic motif was also present on the ovarian cancer cell membranes, and not only secreted into the ascites. Among unsulfated core 1 structures (major components) and core 2 structures (minor components) (Karlsson et al. 2004), low-intense ions corresponding to the trisialylated core 1 structure were detected and the MS/MS confirmed the presence of the disialic motif (Figure 5). This structure has the same sequence as the core 1 *O*-linked oligosaccharide containing the disialic acid motif identified on human glycophorin (Fukuda et al. 1987).

Downloaded from https://academic.oup.com/glycob/article/22/7/918/1988054 by guest on 21 August 2022

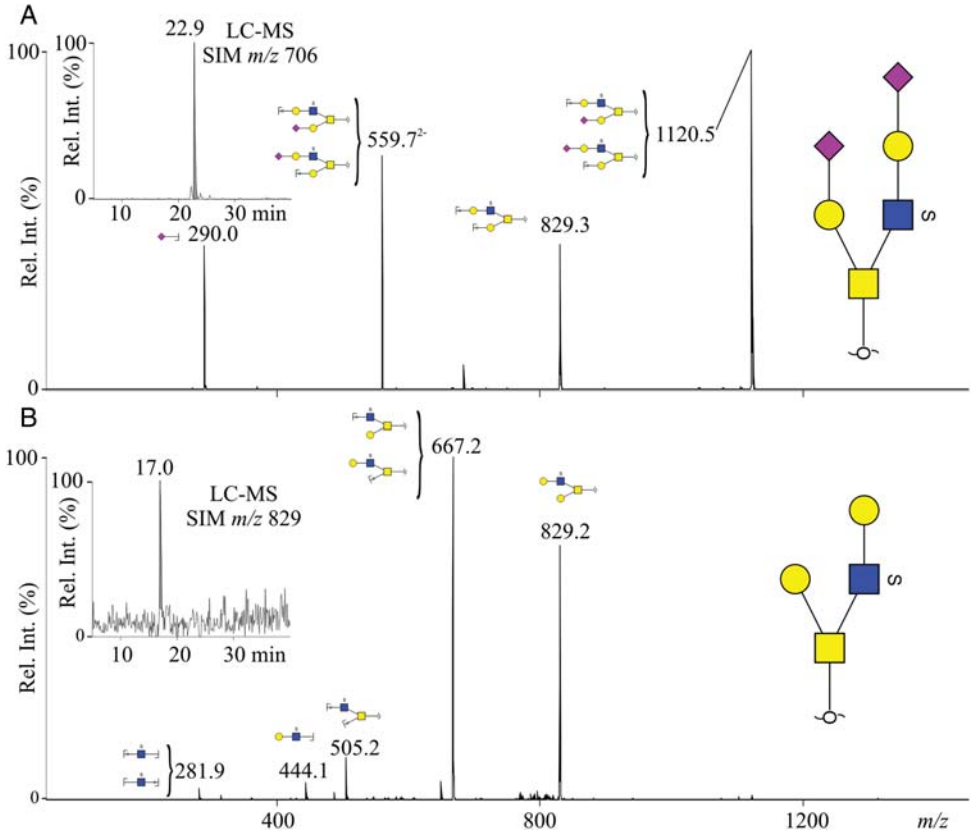

Fig. 3. Identification of sulfated sialylated core 2 structure NeuAc2-Gal1-4(HSO_3-)GlcNAc1-6(NeuAc2-Gal1-3)GalNAcol from ovarian ascites. The MS/MS spectrum of the $[M–2H]^{2–}$ ion of *m/z* 706 eluted at retention time (RT) 22.9 min before (**A**) and that of the $[M–H]^{–}$ ion of *m/z* 829 eluted at RT 17.0 min after (**B**) desialylation. Inserted are selected ion chromatograms of each ion, respectively. Key to symbols, see Figure 2.

Identification of O-linked fucose-type oligosaccharide

Although there was no indication of fucose linked to mucin-type *O*-linked structures, another type of fucosylation was detected. Low-intense $[M–H]^{–}$ ions with *m/z* 530 and 821 were detected (Table I) among the mucin-type oligosaccharides released by reductive β-elimination. The lower mass corresponded to a composition of an alditol with one fucose, one hexose and one *N*-acetylhexosamine (HexNAc), whereas the higher was the sialylated version of this. Closer examination of the LC-MS/MS spectrum of the $[M–H]^{–}$ ions with *m/z* 530 (Figure 6) identified the structure. Despite the low intensity of this parent ion providing noisy fragmentation data, the fucose could be deduced to be located at the reducing end as a fucitol. Abundant fragment ions from the fragmentation of glycosidic linkages could be identified, providing a collision spectrum previously reported for the sequence Hex-HexNAc-Fucitol (Wilson et al. 2008), despite the presence of high-abundant unassigned ions (i.e. *m/z* 327.0, 339.1 and 415.9), believed to be due to the background noise. The assignment of this structure showed that not only *O*-linked mucin-type oligosaccharides were present, but also the epidermal growth factor (EGF)-type *O*-linked fucose (Luther and Haltiwanger 2009), which is usually found attached to low-mass proteins containing EGF domains. However, it has also been shown to be present on high-molecular-mass proteins in human breast milk fat globular membranes and its sialylated version in bovine milk (Wilson et al. 2008). The identification of the unsialylated structure in the fraction of high-molecular-mass acidic proteins in ascites indicates that despite not being negatively charged itself, it must be associated with an acidic protein carrier. This suggests that the proteins carrying this epitope also are likely to carry high amounts of sialic acid and sulfate, present on proteins such as mucins or proteoglycans. So far, the consensus sequence for *O*-linked fucose has not been found to be present within EGF domains of mucins, but it is present in some proteoglycans (see section *Identification of proteoglycan core proteins in ovarian cancer ascites*).

Screening of oligosaccharide epitopes in ovarian cancer samples

Having identified both core 1 and 2 structures in human ascites, additional ovarian cancer ascites samples were screened for these types of oligosaccharides by LC-MS, and it was found that the dominating structures identified in the original sample were also found in all the additional samples (Table II). This shows that the core 1 and 2 structures are ubiquitous in ovarian cancer ascites. In order to investigate the

Downloaded from https://academic.oup.com/glycob/article/22/7/918/1988054 by guest on 21 August 2022

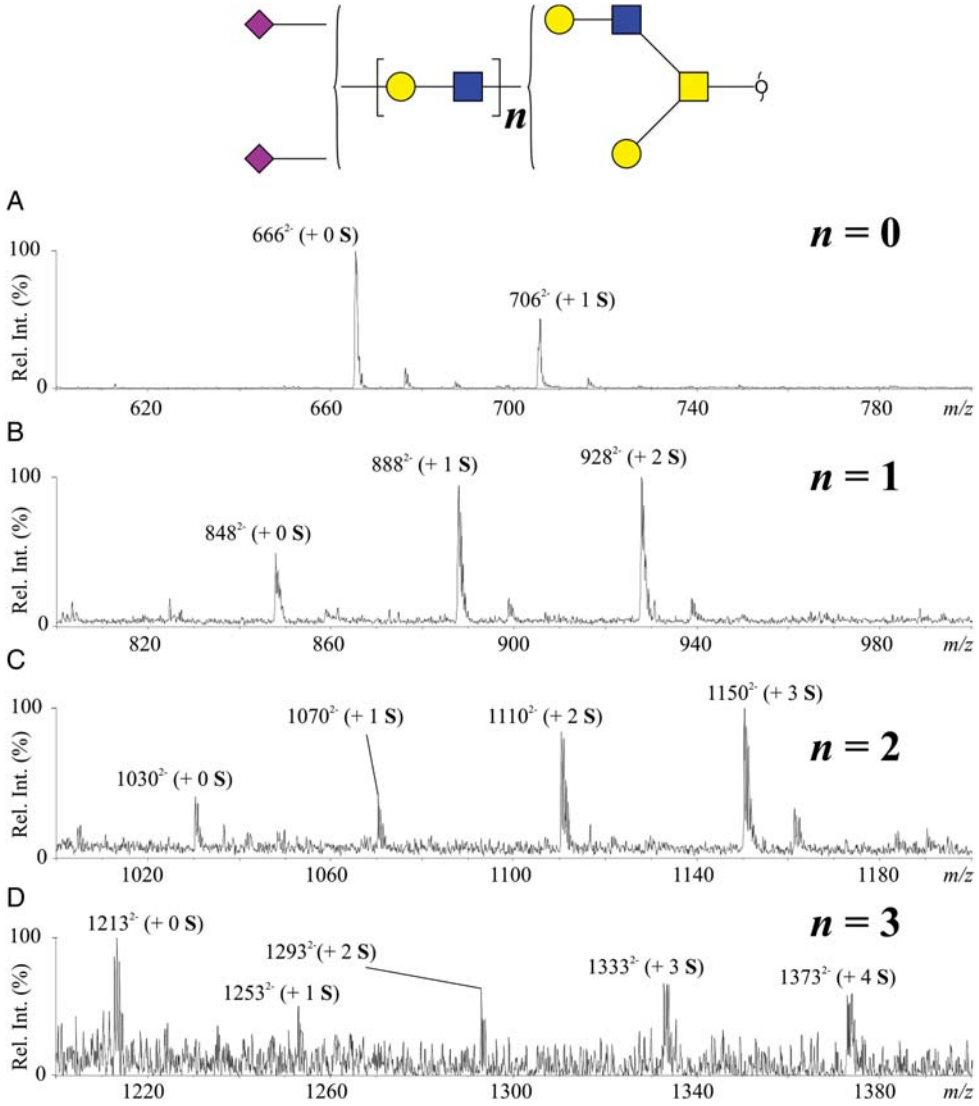

Fig. 4. Sulfation of human ascites *O*-linked oligosaccharides. Extension of sulfated core 2 structures with various amount ($n = 0–3$) of LacNAc units as detected as $[M–2H]^{2-}$ ions detected by LC-MS with no LacNAc (**A**) between retention time (RT) 19.2 and 31.8 min, one LacNAc (**B**) between RT 24.8 and 30.5 min, two LacNAcs (**C**) between RT 29.9 and 33.6 min and three LacNAcs (**D**) between RT 35.4 and 36.5 min. Key to symbols, see Figure 2. RT refers to the chromatogram in Figure 1B.

incidence of sulfation, the $[M–H]^-$ ion of *m/z* 1120 (Galβ1-3(Galβ1-4(HSO_3-6)GlcNAcβ1-6)GalNAcol + NeuAc) was also screened in all the samples. This showed that also sulfation was a common feature of the ovarian cancer ascites, since it was successfully detected in 18 of the 20 samples analyzed. In the remaining two, the presence of sulfated oligosaccharides cannot be ruled out, since the overall MS signal of oligosaccharides in these two samples were low, rendering the detection of sulfated oligosaccharides to be below the detection limit.

CA125/MUC16 in ovarian cancer ascites

Since CA125/MUC16 is a common mucin marker for ovarian cancer, it was investigated how the identified oligosaccharides were connected to CA125. In 17 of the 24 samples investigated, CA125 activity was detected in the high-molecular-mass region >1 MDa after SDS–AgPAGE and western blotting (Table II and Supplementary data, Figure S1). Samples with absent, low and high CA125 activity were also subjected to in-gel digestion and LC-MS/MS identification using a protein database consisting of known human mucins, in order to specifically identify mucins in the samples. In four samples, we found peptides from mucin apoproteins (MUC16, MUC5B and MUC1; Table II and Supplementary data, Table S3). The highest incidence of peptides was a patient diagnosed with benign serous cystadenoma, where both MUC5B (five peptides) and MUC16 (eight peptides) were identified. This patient was also found to have the highest amount of CA125/MUC16 activity by western blotting. In one sample, MUC16 was identified by LC-MS, where there was no CA125 immunoreactivity. MUC1 (two

Downloaded from https://academic.oup.com/glycob/article/22/7/918/1988054 by guest on 21 August 2022

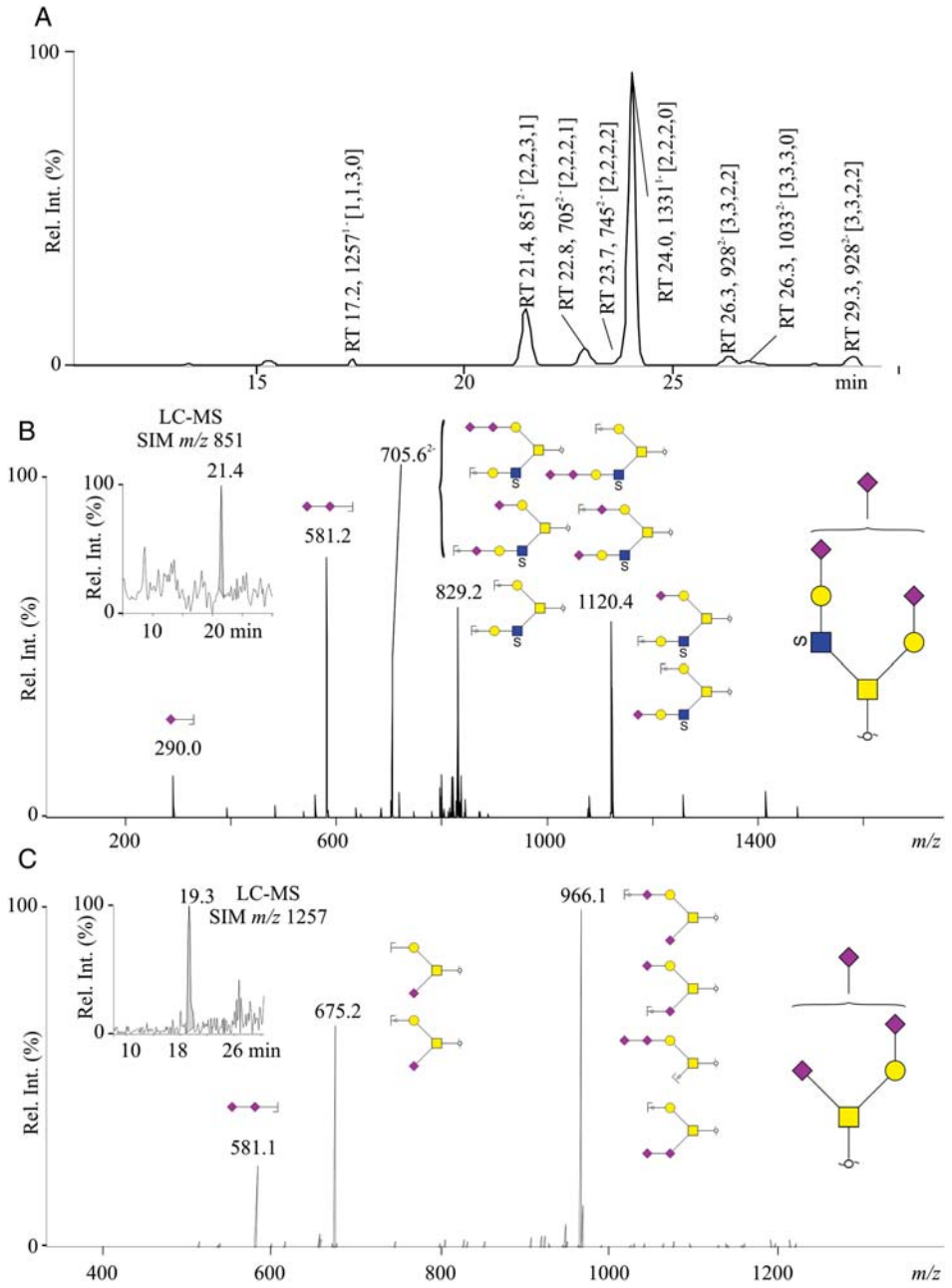

Fig. 5. Disialic acid in human ovarian cancer ascites and tissue. Selected ion chromatogram of the C_2-type fragment of 581 (NeuAc-NeuAc-) showing that the disialylated motif is frequently found among the *O*-linked oligosaccharides from the ascites samples (**A**). MS/MS of the sulfated trisialylated core 2 structure NeuAc2-Gal1-4(HSO_3-)GlcNAc1-6(NeuAc2-Gal1-3)GalNAcol + NeuAc with an $[M–2H]^{2–}$ ion of *m/z* 851 eluted at retention time (RT) 21.4 min from the ascites sample (**B**) and the MS/MS spectrum of the $[M–H]^–$ ion of *m/z* 1257 eluted at RT 19.4 min released from the membrane fraction of ascites cancer tissue. Inserted are selected ion chromatograms of each ion from ascites (B) and cancer tissue (**C**), respectively. Oligosaccharide alditol compositions are referred to as (Hex, HexNAc, NeuAc, sulfate).

peptides) was also found in one patient diagnosed with papillary serous cystadenocarcinoma. Mucins are usually difficult to digest with trypsin and other proteases due to their extensive glycosylation. This has been shown for instance for MUC16 isolated from an ovarian cancer cell line (Yin and Lloyd 2001). The higher sensitivity of western blotting compared with LC-MS can explain the discrepancy between techniques for the detection of CA125/MUC16. This indicates that also the other mucins detected by LC-MS will be more consistently detected by western blotting.

Identification of proteoglycan core proteins in ovarian cancer ascites

In the proteomic analysis, it was found that peptides matched to apomucins only corresponded to a minor fraction of all

Downloaded from https://academic.oup.com/glycob/article/22/7/918/1988054 by guest on 21 August 2022

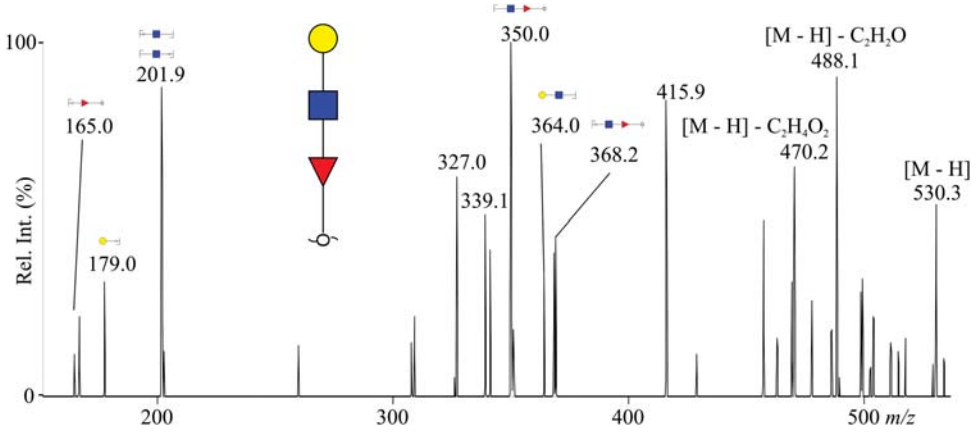

Fig. 6. *O*-Linked fucose in human ovarian cancer tissue. The MS/MS spectrum of the structure Gal-GlcNAc-Fucol with an $[M–H]^-$ ion of *m/z* 530 eluted at retention time 17.5 min from the ascites sample.

Table II. Identification of mucins and mucin oligosaccharides from ascites from human ovarian cancer patients

Mucin oligosaccharide and mucin apoprotein	Incidence
Oligosaccharide motif	
Core 1	100% (22/22)
Core 2	100% (22/22)
Sulfate	91% (20/22)
Apomucin	
MUC16 western	71% (17/24)
MUC16 LC-MS	50% (3/6)
MUC1	17% (1/6)
MUC5B	17% (1/6)

peptides identified in the total acidic fraction. Analysis of the acidic proteins from human ascites from patients with ovarian cancer indicated that the mucin component of the sample is often only a minor constituent. In the sample analyzed thoroughly for glycosylation (Figure 1), we found that there were significant *O*-linked glycosylation, without any major mucin apoprotein identified by LC-MS or by western blotting (MUC16). The presence of KS-like sulfation indicated that one potential candidate for the presence of sulfated *O*-linked oligosaccharides is that they are attached to KS proteoglycan-type apoproteins. High-molecular-mass proteins from three of the samples were separated by SDS–AgPAGE and the area from 100 kDa to 2 MDa was cut into pieces. After trypsin digestion and LC-MS/MS of pieces cut out after SDS–AgPAGE, 10 proteoglycan-type apoproteins were identified, together with a large number of additional acidic proteins identified by their peptides (Table III). Interrogating the UniProt database to ascertain whether these proteins are known to contain *O*-linked oligosaccharides, only identified lumican to have consistently been shown to contain *O*-linked KS. However, proteins, such as agrin, versican and dystroglycan, contain extended stretches in their amino acid sequence rich in serine, threonine and proline, where extensive *O*-linked glycosylation is expected. This makes them potential candidates for the sulfated and unsulfated *O*-linked oligosaccharides identified in the samples, in addition to the mucins identified in Table II.

Discussion

Identification and characterization of high-molecular-weight acidic proteins from ovarian ascites from patients using SDS–AgPAGE provides a platform complementary to two-dimensional SDS–PAGE for biomarker discovery in this disease. Although mucins are believed to play an important role in ovarian cancer (e.g. CA125 and CA19-9), their importance may not necessarily be reflected in their abundances in ascites. Furthermore, their use as diagnostic markers could relate more to their immunogenicity and the historical use of antibodies and not MS to identify and measure markers. Mucins are not normally found at high concentrations in serum and hence serve as good markers in cancer.

The detection of acidic proteins by Alcian blue provided distinct bands by SDS–AgPAGE, and most likely these bands consist of traditional mucins as well as mucin-type proteoglycans with short KS oligosaccharides. Identification of proteins in this high-molecular-weight region suggests that there are several candidates other than mucins that carry *O*-linked glycans (Table III). From the estimated size of classical *O*-linked KS chains (KSII) from articular cartilage, the number of LacNAc repeats detected here (Figure 4) is in the low end of the range (Funderburgh 2000). However, with novel techniques developing for studying glycosylation, distinguishing KSII from sulfated *O*-linked will become arbitrary and the poly-prefix of the LacNAc chain will be converted into a direct and correct display of individual polymer/oligomer chains.

The oligosaccharides from ovarian cancer ascites are in many ways unique compared to other mucin-type oligosaccharides investigated to date. They do not contain any fucose common on the mucins found on mucosal surfaces, often as blood group antigens from the ABO and/or Lewis system. Hence, they are more related to the glycosylation of constitutively highly expressed glycoproteins in human plasma.

Downloaded from https://academic.oup.com/glycob/article/22/7/918/1988054 by guest on 21 August 2022

Table III. Combined proteomic results of high-molecular-weight proteoglycans and proteins identified from human ascites

Protein ID	Common name	*O*-Fuc EGF motif CXXX(A/G/S)(S/T)C	PG modification
Proteoglycans			
Q9NR99	Matrix-remodeling-associated protein 5		No information
O00468	Agrin	x	HS
P21810	Biglycan		DS
P35052	Glypican-1		HS
P51884	Lumican		KS
P98160	Perlecan	x	HS,CS
Q14118	Dystroglycan	x	No info
P13611	Versican		CS
Q99715	Collagen α-1(XII)		CS
P02760	AMBP protein precursor		CS
Other proteins			
Q8IUX7	Adipocyte enhancer-binding protein 1		
P01011	α-1-antichymotrypsin		
P01023	α-2-macroglobulin		
Q06481	Amyloid-like protein 2		
P04114	Apolipoprotein B-100		
P49747	Cartilage oligomeric matrix protein		
P02741	C-reactive protein		
P16070	CD44 antigen		
P00450	Ceruloplasmin		
P08709	Coagulation factor VII	x	
P01024	Complement C3		
P0C0L5	Complement C4-B		
P08603	Complement factor H		
P12109	Collagen α-1(VI) chain		
P12111	Collagen α-3(VI) chain	x	
P82279	Crumbs homolog 1		
P11532	Dystrophin		
Q8IUI1	Fibulin 2		
P02679	Fibrinogen γ chain		
P02751	Fibronectin		
Q14520	Hyaluronan-binding protein 2		
P02768	Serum albumin		
p01857	Ig gamma-1 chain C region		
P19827	Inter-α-trypsin inhibitor heavy chain H1		
P19823	Inter-α-trypsin inhibitor heavy chain H2		
Q06033	Inter-α-trypsin inhibitor heavy chain H3		
P07942	Laminin subunit β-1		
Q14766	Latent-transforming growth factor β-binding protein 1	x	
Q68BL8	Olfactomedin-like protein 2B		
p05155	Plasma protease C1 inhibitor		
Q9Y4D7	Plexin-D1	x	
Q4LDE5	Sushi, von Willebrand factor type A, EGF and pentraxin domain-containing protein 1	x	
P35442	Thrombospondin-2		
P35443	Thrombospondin-4		
Q9P1Z9	Uncharacterized protein KIAA1529		
p02774	Vitamin D-binding protein		
p04004	Vitronectin		

HS, heparan sulfate; DS, dermatan sulfate; KS, keratan sulfate; CS, chondroitin sulfate. x means present.

Downloaded from https://academic.oup.com/glycob/article/22/7/918/1988054 by guest on 21 August 2022

Functionally, this could be related to the non-mucosal nature of the mesothelial/ovarian surface, i.e. it is internal rather than exposed to microbial flora. However, the sulfation of plasma glycoproteins is rare. The lack of fucosylation is also likely to make the detected oligosaccharides a poor target for L-selectin, or any of the other selectins (McEver 1997). Other lectins targeting sulfated compounds, such as siglec-8 (Hudson et al. 2009) and galectin-8 (Ideo et al. 2011), also have different additional structural requirements to what we report in ovarian cancer. This indicates that the sulfation of ascites fluid in ovarian cancer represent a novel biological function. If this function has an effect on the cancer development, oligosaccharide sulfation may serve as a diagnostics for ovarian cancer detection or for monitoring ovarian cancer therapies.

In regard to the other "exotic" oligosaccharide epitopes, the potential EGF-type glycosylation still needs further investigation. Many of the proteoglycan candidates in Table III contains EGF domains and also the specific *O*-fucose consensus sequence, making them potential candidates to carry *O*-linked fucose oligosaccharides, and explain why *O*-linked fucose was found among high-molecular-weight acidic glycoproteins.

The disialic acid epitopes could also represent an interesting opportunity as a biomarker and give insight into the cancer progression. The ability of ovarian mucin-type oligosaccharides to bind to siglecs (Crocker and Varki 2001) is still unexplored. In particular, Siglec-7 has been found to bind the disialic acid motif (Nicoll et al. 2003). Binding to Siglec-7 could influence cancer progression by protecting from immune surveillance by natural killer (NK) cells expressing Siglec-7. Disialic acid motifs are frequently detected among glycosphingolipids, but less so among *O*- or *N*-linked oligosaccharides. Since the late pathway for the glycosylation of both *N*-linked, *O*-linked and glycosphingolipids are believed to utilize the same glycosylation machinery and enzymes, it is more than likely that the disialic acid motif is more ubiquitous among glycoproteins than expected previously. The analytical techniques for glycomics such as permethylation and MS (Kang et al. 2008; North et al. 2009; Prien et al. 2010) as well as the LC-MS of underivatized oligosaccharides as presented here have now reached the sophistication to identify this epitope on a more regular basis.

The data also indicate that *O*-linked KS is a significant component of the ovarian cancer ascites. This opens up the possibility to explore proteoglycans with extended mucin domains, such as lumican, agrin, versican and dystroglycan, for their role in ovarian cancer. Dystroglycan has also been shown to contain not only mucin-type *O*-linked oligosaccharides, but also *O*-mannose initiated oligosaccharides within its mucin domain (Stalnaker et al. 2011). The MS/MS fragmentation positively confirmed the presence of reduced HexNAc (GalNAc) and deoxyhexose (Fuc), and the absence of reduced Hex (Man) showed that *O*-linked Man can only be a very minor contributor to the *O*-linked glycome in human ascites. The data in this report also show that additional proteoglycans are present, where only limited information about these types of molecules in ovarian tissue and their role in the biology of ovarian cancer are currently available. Accumulation of ascites fluid in ovarian cancer patients is due to shed ovarian cancer cells blocking the lymphatic drainage of the peritoneal cavity. The ectopic presence of mucins is a direct consequence of secretion directly into the peritoneal fluid. An increased amount of ascites can also more rarely occur in benign ovarian tumors, but in healthy individuals large volumes of fluid transit rapidly through the peritoneum. This investigation did not reveal any obvious qualitative differences between different subtypes of ovarian cancer or with benign disease (summarized in Supplementary data, Table S3), neither in respect of the type of mucins and their glycosylation nor the type of proteoglycans present. Instead, it provides a roadmap for quantitative analysis of the target molecule for further investigation. In order to further investigate the role of proteoglycans in ovarian cancer, glycomic and glycoprotemic analyses of cystic fluid and tumor tissue, where the cancer-related proteins are enriched, are likely to provide information about the origin of the proteoglycans and their role in ovarian cancer development.

Materials and methods

Enrichment of mucin-type oligosaccharides

Human ascites samples (0.5–1.0 mL) were diluted ×10 with 250 mM sodium chloride in 20 mM Tris/10 mM ethylenediaminetetraacetic acid (EDTA), 50 µL of protease inhibitors was added and the samples (Supplementary data, Tables S1 and S2) were injected to a diethylaminoethyl fast flow (DEAE FF) (1 mL) column (GE Healthcare, Uppsala, Sweden) run at 1.0 mL/min in the same solution. After loading (5–10 min), the columns were washed with 10 mL of the starting buffer and the retarded fraction was collected (10 mL) by increasing the sodium chloride concentration to 1.0 M. The proteins in the collected samples were precipitated with ethanol (80% final concentration) at −20°C for 12 h.

SDS–AgPAGE and SDS–PAGE

The acidic fraction from ascites were reduced in SDS–AgPAGE sample buffer in 10 mM dithiothreitol (DTT) at 95° C for 10 min and then alkylated with iodoacetamide (25 mM) for 1 h at room temperature. Samples was loaded (2–20 µL) and electrophoresed (Schulz et al. 2002), blotted onto polyvinylidene fluoride (PVDF) membranes and stained with Alcian blue (Schulz et al. 2002) or developed by western blotting.

Identification of high-molecular-weight acidic glycoproteins from human ascites

Protein identification was performed after tryptic digestion of proteins found in the region between 100 kDa and 2 MDa using LC-electrospray-MS/MS. (ThermoFinnigan, San Jose, CA). SEQUEST (fragmented peptide ion pattern matching, ThermoFinnigan) were used for database searching and protein identification using either the Uniprot human database or a smaller database of human mucins (MUC1–20) (http://www.medkem.gu.se/mucinbiology/). Positive protein matches were assigned according to the criteria of at least two peptide sequences with the manual inspection of tandem mass spectra showing at least four consecutive *b* or *y* overlapping ions, an X_{corr} of >2.0 and a ΔC_n of >0.1.

Glycoprotein oligosaccharide profiling

Mucin glycosylation is predominantly *O*-linked and can constitute up to 80% of the total mucin molecular weight. *O*-Linked oligosaccharides were released from blots after separation using SDS–AgPAGE using reductive β-elimination as described (Schulz et al. 2002) and analyzed by LC-MS/MS using graphitized carbon chromatography (7 µL/min in a 300-µm ID × 100 mm column with 5 µm particles) and a gradient of water-acetonitrile in 10 mM ammonium bicarbonate. Oligosaccharides were injected (5 µL of a total of 10 µL) and detected with an Agilent XCT ion trap mass spectrometer (Santa Clara, CA) run in a negative mode, with smart fragmentation (90–120%) of the two most intense ions in each full scan. The remaining 5 µL of oligosaccharides were desialylated using 10 mU sialidase A (α2-3, α2-6, α2-8 and α2-9 specific) (Glyko, Novato, CA) according to the manufacturers' recommendation and incubated at 37°C for 16 h. The sample was desalted on homemade micro desalting columns (~2 µL) containing Carbograph material (Alltech, Deerfield, IL) laid on the top of a reverse-phase µ-C18 ZipTip (Millipore, Bedford, MA; Karlsson et al. 2004) and subjected to LC-MS and LC-MS/MS as described in the beginning of this section. Detected oligosaccharides were sequenced based on the MS/

Downloaded from https://academic.oup.com/glycob/article/22/7/918/1988054 by guest on 21 August 2022

MS spectra and core-type linkage configuration were assumed based on cores 1–3, based on the substitution pattern of the reducing end GalNAcol and comparison with reference MS/MS spectra. Sialic acid was assumed to be 6–linked, if it was found to be directly linked to the GalNAcol residue. Sulfation of the core 2 inner core was found to be on 6-position due to the positive identification of sulfated HexNAc. Sulfation further out of the LacNAc chain was not verified. The type 2 chain was assumed based on the positive identification of cross-ring fragments specific for the C-4 extension of HexNAc (Schulz et al. 2002). Structures and associated fragment spectra were submitted to the Unicarb-DB depository (Hayes et al. 2011).

Western blotting

Human ascites blotted onto PVDF membranes was blocked in 1% bovine serum albumin in Tris-buffered saline-Tween (TBS-T) overnight at 4°C. The samples was then incubated with ab1107 (CA125/MUC16, 1/10,000) in the same buffer for 3 h and washed 3 × 10 min with TBS-T, before incubating (1 h) with horseradish peroxidase-labeled secondary antibody (1/10,000 for ab1107, 1/1000 for the other) in blocking solution. The blots were washed 5 × 20 min with TBS-T and developed using the western femto reagent (Pierce, Rockford, IL).

Supplementary data

Supplementary data for this article is available online at http://glycob.oxfordjournals.org/.

Funding

This study was in part funded the EU Marie Curie Programme PIRG-GA-2007-205302 and the Swedish Research Council (621-2010-5322). M.A.M. is supported by a Senior Research Fellowship from the Australian National Health and Medical Research Council.

Conflict of interest

None declared.

Abbreviations

DEAE FF, diethylaminoethyl fast flow; DTT, dithiothreitol; EDTA, ethylenediaminetetraacetic acid; EGF, epidermal growth factor; ER, endoplasmic reticulum; Hex, hexose; HexNAc, *N*-acetylhexosamine; KS, keratan sulfate; LacNAc, *N*-acetyllactosamine; LC, liquid chromatography; MS/MS, Tandem mass spectrometry; NK, natural killer; PVDF, polyvinylidene fluoride; SDS–AgPAGE, sodium dodecyl sulfate–polyacrylamide/agarose composite gel electrophoresis; TBS, tris-buffered saline; TBS-T, TBS-Tween.

References

Axelsson MA, Karlsson NG, Steel DM, Ouwendijk J, Nilsson T, Hansson GC. 2001. Neutralization of pH in the Golgi apparatus causes redistribution of glycosyltransferases and changes in the *O*-glycosylation of mucins. *Glycobiology*. 11(8):633–644.

Brockhausen I. 2006. Mucin-type *O*-glycans in human colon and breast cancer: Glycodynamics and functions. *EMBO Rep*. 7(6):599–604.

Chauhan SC, Kumar D, Jaggi M. 2009. Mucins in ovarian cancer diagnosis and therapy. *J Ovarian Res*. 2:21.

Crocker PR, Varki A. 2001. Siglecs in the immune system. *Immunology*. 103 (2):137–145.

Estrella RP, Whitelock JM, Packer NH, Karlsson NG. 2010. The glycosylation of human synovial lubricin: Implications for its role in inflammation. *Biochem J*. 429(2):359–367.

Fukuda M, Lauffenburger M, Sasaki H, Rogers ME, Dell A. 1987. Structures of novel sialylated *O*-linked oligosaccharides isolated from human erythrocyte glycophorins. *J Biol Chem*. 262(25):11952–11957.

Funderburgh JL. 2000. Keratan sulfate: Structure, biosynthesis, and function. *Glycobiology*. 10(10):951–958.

Gill DJ, Chia J, Senewiratne J, Bard F. 2010. Regulation of *O*-glycosylation through Golgi-to-ER relocation of initiation enzymes. *J Cell Biol*. 189 (5):843–858.

Hayes CA, Karlsson NG, Struwe WB, Lisacek F, Rudd PM, Packer NH, Campbell MP. 2011. UniCarb-DB: A database resource for glycomic discovery. *Bioinformatics*. 27(9):1343–1344.

Holmén JM, Karlsson NG, Abdullah LH, Randell SH, Sheehan JK, Hansson GC, Davis CW. 2004. Mucins and their *O*-Glycans from human bronchial epithelial cell cultures. *Am J Physiol Lung Cell Mol Physiol*. 287(4): L824–L834.

Hudson SA, Bovin NV, Schnaar RL, Crocker PR, Bochner BS. 2009. Eosinophil-selective binding and proapoptotic effect in vitro of a synthetic Siglec-8 ligand, polymeric 6′-sulfated sialyl Lewis x. *J Pharmacol Exp Ther*. 330(2):608–612.

Ideo H, Matsuzaka T, Nonaka T, Seko A, Yamashita K. 2011. Galectin-8-N-domain recognition mechanism for sialylated and sulfated glycans. *J Biol Chem*. 286(13):11346–11355.

Kang P, Mechref Y, Novotny MV. 2008. High-throughput solid-phase permethylation of glycans prior to mass spectrometry. *Rapid Commun Mass Spectrom*. 22(5):721–734.

Karam AK, Karlan BY. 2010. Ovarian cancer: The duplicity of CA125 measurement. *Nat Rev Clin Oncol*. 7(6):335–339.

Karlsson NG, Wilson NL, Wirth HJ, Dawes P, Joshi H, Packer NH. 2004. Negative ion graphitised carbon nano-liquid chromatography/mass spectrometry increases sensitivity for glycoprotein oligosaccharide analysis. *Rapid Commun Mass Spectrom*. 18(19):2282–2292.

Kui Wong N, Easton RL, Panico M, Sutton-Smith M, Morrison JC, Lattanzio FA, Morris HR, Clark GF, Dell A, Patankar MS. 2003. Characterization of the oligosaccharides associated with the human ovarian tumor marker CA125. *J Biol Chem*. 278(31):28619–28634.

Larsson JM, Karlsson H, Crespo JG, Johansson ME, Eklund L, Sjövall H, Hansson GC. 2011. Altered *O*-glycosylation profile of MUC2 mucin occurs in active ulcerative colitis and is associated with increased inflammation. *Inflamm Bowel Dis*. 17(11):2299–2307.

Lindén SK, Sutton P, Karlsson NG, Korolik V, McGuckin MA. 2008. Mucins in the mucosal barrier to infection. *Mucosal Immunol*. 1(3):183–197.

Luther KB, Haltiwanger RS. 2009. Role of unusual *O*-glycans in intercellular signaling. *Int J Biochem Cell Biol*. 41(5):1011–1024.

McEver RP. 1997. Selectin-carbohydrate interactions during inflammation and metastasis. *Glycoconj J*. 14(5):585–591.

Nicoll G, Avril T, Lock K, Furukawa K, Bovin N, Crocker PR. 2003. Ganglioside GD3 expression on target cells can modulate NK cell cytotoxicity via siglec-7-dependent and -independent mechanisms. *Eur J Immunol*. 33(6):1642–1648.

North SJ, Hitchen PG, Haslam SM, Dell A. 2009. Mass spectrometry in the analysis of *N*-linked and *O*-linked glycans. *Curr Opin Struct Biol*. 19 (5):498–506.

Pang PC, Chiu PC, Lee CL, Chang LY, Panico M, Morris HR, Haslam SM, Khoo KH, Clark GF, Yeung WS, et al. 2011. Human sperm binding is mediated by the sialyl-Lewis(x) oligosaccharide on the zona pellucida. *Science*. 333(6050):1761–1764.

Pedersen SK, Harry JL, Sebastian L, Baker J, Traini MD, McCarthy JT, Manoharan A, Wilkins MR, Gooley AA, Righetti PG, et al. 2003. Unseen

Downloaded from https://academic.oup.com/glycob/article/22/7/918/1988054 by guest on 21 August 2022

proteome: Mining below the tip of the iceberg to find low abundance and membrane proteins. *J Proteome Res*. 2(3):303–311.

Prien JM, Prater BD, Cockrill SL. 2010. A multi-method approach toward de novo glycan characterization: A Man-5 case study. *Glycobiology.* 20 (5):629–647.

Saldova R, Wormald MR, Dwek RA, Rudd PM. 2008. Glycosylation changes on serum glycoproteins in ovarian cancer may contribute to disease pathogenesis. *Dis Markers*. 25(4–5):219–232.

Schulz BL, Packer NH, Karlsson NG. 2002. Small-scale analysis of *O*-linked oligosaccharides from glycoproteins and mucins separated by gel electrophoresis. *Anal Chem*. 74(23):6088–6097.

Schulz BL, Sloane AJ, Robinson LJ, Prasad SS, Lindner RA, Robinson M, Bye PT, Nielson DW, Harry JL, Packer NH, et al. 2007. Glycosylation of sputum mucins is altered in cystic fibrosis patients. *Glycobiology.* 17 (7):698–712.

Schulz BL, Sloane AJ, Robinson LJ, Sebastian LT, Glanville AR, Song Y, Verkman AS, Harry JL, Packer NH, Karlsson NG. 2004. Mucin glycosylation changes in cystic fibrosis lung disease are not manifest in submucosal gland secretions. *Biochem J*. 387:911–919.

Stalnaker SH, Stuart R, Wells L. 2011. Mammalian *O*-mannosylation: Unsolved questions of structure/function. *Curr Opin Struct Biol*. 21(5):603–609.

Tarp MA, Clausen H. 2008. Mucin-type *O*-glycosylation and its potential use in drug and vaccine development. *Biochim Biophys Acta*. 1780(3):546–563.

Thomsson KA, Schulz BL, Packer NH, Karlsson NG. 2005. MUC5B glycosylation in human saliva reflects blood group and secretor status. *Glycobiology.* 15(8):791–804.

Wilson NL, Robinson LJ, Donnet A, Bovetto L, Packer NH, Karlsson NG. 2008. Glycoproteomics of milk: Differences in sugar epitopes on human and bovine milk fat globule membranes. *J Proteome Res*. 7 (9):3687–3696.

Wilson NL, Schulz BL, Karlsson NG, Packer NH. 2002. Sequential analysis of *N*- and *O*-linked glycosylation of 2D-PAGE separated glycoproteins. *J Proteome Res*. 1(6):521–529.

Yin BW, Lloyd KO. 2001. Molecular cloning of the CA125 ovarian cancer antigen: Identification as a new mucin, MUC16. *J Biol Chem*. 276 (29):27371–27375.

Zaia J. 2009. On-line separations combined with MS for analysis of glycosaminoglycans. *Mass Spectrom Rev.* 28(2):254–272.

Downloaded from https://academic.oup.com/glycob/article/22/7/918/1988054 by guest on 21 August 2022